Human Molecular Genetics, 2016, Vol. 25, No. 18 3925–3936

doi: 10.1093/hmg/ddw233
Advance Access Publication Date: 27 July 2016
Original Article

ORIGINAL ARTICLE

SOX10 regulates an alternative promoter at the Charcot-Marie-Tooth disease locus *MTMR2*

Elizabeth A. Fogarty[1,†], Megan H. Brewer[2,†], Jose F. Rodriguez-Molina[3], William D. Law[2], Ki H. Ma[3], Noah M. Steinberg[2], John Svaren[4,5] and Anthony Antonellis[1,2,6,*]

[1]Neuroscience Graduate Program, [2]Department of Human Genetics, University of Michigan, Ann Arbor, MI, USA, [3]Cellular and Molecular Pathology (CMP) Program, [4]Waisman Center, [5]Department of Comparative Biosciences, University of Wisconsin-Madison, Madison, WI, USA and [6]Department of Neurology, University of Michigan, Ann Arbor, MI, USA

*To whom correspondence should be addressed at: University of Michigan, 3710A Medical Sciences II, 1241 E. Catherine St. SPC 5618 Ann Arbor, MI, USA. Tel: +1-734-647-4058; FAX: +1-734-763 3784; Email: antonell@umich.edu

Abstract

Schwann cells are the myelinating glia of the peripheral nervous system and dysfunction of these cells causes motor and sensory peripheral neuropathy. The transcription factor SOX10 is critical for Schwann cell development and maintenance, and many SOX10 target genes encode proteins required for Schwann cell function. Loss-of-function mutations in the gene encoding myotubularin-related protein 2 (*MTMR2*) cause Charcot-Marie-Tooth disease type 4B1 (CMT4B1), a severe demyelinating peripheral neuropathy characterized by myelin outfoldings along peripheral nerves. Previous reports indicate that *MTMR2* is ubiquitously expressed making it unclear how loss of this gene causes a Schwann cell-specific phenotype. To address this, we performed computational and functional analyses at *MTMR2* to identify transcriptional regulatory elements important for Schwann cell expression. Through these efforts, we identified an alternative, SOX10-responsive promoter at *MTMR2* that displays strong regulatory activity in immortalized rat Schwann (S16) cells. This promoter directs transcription of a previously unidentified *MTMR2* transcript that is enriched in mouse Schwann cells compared to immortalized mouse motor neurons (MN-1), and is predicted to encode an N-terminally truncated protein isoform. The expression of the endogenous transcript is induced in a heterologous cell line by ectopically expressing SOX10, and is nearly ablated in Schwann cells by impairing SOX10 function. Intriguingly, overexpressing the two MTMR2 protein isoforms in HeLa cells revealed that both localize to nuclear puncta and the shorter isoform displays higher nuclear localization compared to the longer isoform. Combined, our data warrant further investigation of the truncated MTMR2 protein isoform in Schwann cells and in CMT4B1 pathogenesis.

Introduction

Charcot-Marie-Tooth (CMT) disease is a heterogeneous group of disorders that represents the most common class of inherited peripheral neuropathies. Patients with CMT disease show varying degrees of muscle weakness and sensory loss in the extremities (1). CMT disease is broadly categorized into two types; axonal CMT (CMT2) is caused by a primary defect in peripheral neurons, whereas demyelinating CMT (CMT1) arises from a primary defect in Schwann cells (2,3). Schwann cells—the myelinating cells of the peripheral nervous system—produce a myelin sheath that allows saltatory conduction along axons. For a recent review of Schwann cell development and myelination, see Monk et al. 2015 (4). Consistent with a defect in

[†]These authors contributed equally to this manuscript
Received: April 6, 2016. **Revised:** June 21, 2016. **Accepted:** July 11, 2016

these cells, patients with CMT1 typically present with slow nerve conduction velocities (5). CMT1 often manifests early in life, with onset by 10 years of age in more than 60% of patients (5), and can be debilitating to the point of rendering patients wheelchair-bound. To date, over 80 genes have been implicated in CMT disease with over 20 implicated in demyelinating forms (CMT1) (6). Genes mutated in CMT1 include those encoding myelin proteins (*e.g. MPZ*) (7) and others with known functions in Schwann cells (*e.g. EGR2*) (8), but many have poorly understood roles in Schwann cell biology. Furthermore, there is no effective treatment for CMT disease, which will likely require gene- and mutation-specific therapies. Thus, characterizing the genes associated with CMT1 will provide a better understanding of Schwann cell physiology and the pathology of demyelinating neuropathies.

Loss-of-function mutations in the myotubularin-related protein 2 (*MTMR2*) gene cause CMT4B1 (OMIM #601382), an autosomal recessive, demyelinating CMT disease distinguished by myelin outfoldings in the peripheral nerves (9). CMT4B1 is particularly severe, as both proximal and distal limbs are affected and symptoms begin at ~34 months of age (10). Consistent with the Schwann cell-specific phenotype in CMT4B1 patients, studies have shown an important role for MTMR2 in Schwann cell biology. In mice, conditional loss of *Mtmr2* in Schwann cells causes neuropathy with myelin outfoldings reminiscent of CMT4B1, whereas the loss of the gene in motor neurons does not cause axonal or myelination phenotypes (11). Furthermore, *Mtmr2* expression is developmentally regulated during peripheral myelination (12), and knock-down of *Mtmr2* in cultured Schwann cells decreases proliferation and increases cell death (13). However, there is evidence that *Mtmr2* is important for neurons *in vivo*, based on genetic interactions between *Mtmr2* and *Fig4* in mouse models of CMT4B1 and CMT4J, respectively (14).

MTMR2 encodes a ubiquitously expressed lipid phosphatase, which converts phosphatidylinositol 3-phosphate (PI(3)P) and PI(3,5)P2 to PI and PI(5)P, respectively (15). The protein contains a PH-GRAM domain, conferring substrate specificity, a PTP catalytic phosphatase domain, a SET-interacting domain (SID), a coiled-coil domain allowing oligomerization, and a PDZ binding domain for protein-protein interactions (16). As such, it is thought that MTMR2 plays a role in membrane trafficking and cell signalling (17). Interestingly, MTMR2 localizes to the nucleus of myelinating and non-myelinating Schwann cells cocultured with sensory neurons (18). However, finer details on the cytoplasmic or nuclear function(s) of MTMR2 remain unclear.

Currently, little is known about the transcriptional regulation of *MTMR2*. Deciphering the regulation of this locus will be important for understanding the function of MTMR2 and will also be particularly salient in determining how the loss of a ubiquitously expressed gene causes a Schwann cell-specific phenotype. Here, we report computational and functional analyses of the *MTMR2* locus, which revealed an alternative, SOX10-dependent promoter; SOX10 is a transcription factor that is essential for all stages of the Schwann cell lineage (19). The activity at this promoter directs the expression of a previously unreported, alternate transcript that encodes an N-terminally truncated protein isoform. Collectively, our findings reveal a SOX10-dependent *MTMR2* gene product in Schwann cells, which should stimulate future studies on the role of MTMR2 protein isoforms in Schwann cells and CMT4B1 pathogenesis.

Results

The MTMR2 locus harbours four putative transcriptional regulatory elements

Multiple-species comparative sequence analysis is a powerful tool for predicting cis-acting transcriptional regulatory elements (20). To identify evolutionarily conserved sequences at *MTMR2*, we scrutinized aligned genomic sequences spanning *MTMR2* and extending to the flanking loci (*MAML2* and *CEP57*) from human, mouse, and chicken using the UCSC Human Genome Browser (http://genome.ucsc.edu/) (21). Specifically, we identified non-coding, non-repetitive genomic sequences that are conserved among these three species. This analysis revealed three multiple-species conserved sequences (MCSs)—two upstream of the predicted transcription start site (TSS) of *MTMR2* and one within the first intron of the major *MTMR2* transcript (Table 1 and Figure 1A). We also included the putative proximal promoter ('Prom1' in Table 1 and Figure 1A) and considered these four genomic segments to be candidate *MTMR2* regulatory elements.

MTMR2-MCS3 displays strong enhancer activity in cultured Schwann cells

To determine if the four candidate regulatory elements described above (Table 1 and Figure 1A) are important for *MTMR2* expression in Schwann cells, we tested each for regulatory potential in S16 cells—a rat immortalized Schwann cell line that expresses myelin-related genes (*e.g. PMP22*, *MPZ*, and *SOX10*) (22–24). Briefly, we cloned each genomic segment upstream of a minimal promoter directing the expression of a firefly luciferase reporter gene (25). Next, we transfected the resulting constructs into cultured S16 cells along with a renilla luciferase expression construct to control for variable cell viability and transfection efficiency. These experiments revealed that *MTMR2*-MCS3 has strong enhancer activity as indicated by a ~22-fold increase in luciferase activity compared to a control vector with no genomic insert (Figure 1B). In contrast, the promoter (Prom1), MCS1, and MCS2 did not dramatically increase luciferase activity above the control expression vector. To determine the specificity of these findings to Schwann cells, we repeated the above experiments in a non-glial cell line (the mouse motor neuron-derived cell line MN-1) (26) that does not express transcription factors important for myelination (*e.g.* SOX10) (24). While *MTMR2*-MCS1 and *MTMR2*-MCS2 showed some activity, none of the elements directed luciferase activity above a 3-fold increase and *MTMR2*-MCS3 displayed less activity than the empty vector (Figure 1C). In sum, these data are consistent with *MTMR2*-MCS3 being important for the transcription of this locus in Schwann cells.

MTMR2-MCS3 is a previously unreported, alternative MTMR2 promoter

Upon scrutinizing *MTMR2*-MCS3 on the UCSC Rat Genome Browser we noted three spliced ESTs (two from brain, one from E11-12 embryos) with 5' ends that overlap the last 75 base pairs of MCS3 (Figure 2A). These findings suggested that *MTMR2*-MCS3 may act as a promoter to express alternative *MTMR2* transcripts. To test this, we performed 5'-rapid amplification of cDNA ends (5'-RACE). Briefly, Mtmr2 cDNA was generated using RNA isolated from cultured rat Schwann (S16) cells and a reverse primer in exon 5. Subsequently, 5'-RACE was performed using reverse primers in exons 4 and 2 of rat *Mtmr2*. The resulting PCR products were cloned and sequenced, and a total of 19 individual clones mapped to the rat *Mtmr2* locus. These studies revealed the presence of two *Mtmr2*-related transcription start sites (Figure 2A). One of these represents the known exon 1 of *Mtmr2* (7 of the 19 sequences map to this first exon; Figure 2A) and the other matches the ESTs that map directly adjacent to, and downstream of, MCS3 (12 of the 19 sequences map to this

Table 1. Putative transcriptional regulatory elements at *MTMR2*

Element ID	Genomic Location[a]	Size (bp)
MTMR2-Prom1	chr11:95,657,371-95,658,478	1,108
MTMR2-MCS1	chr11:95,694,768-95,695,577	810
MTMR2-MCS2	chr11:95,687,566-95,688,075	510
MTMR2-MCS3 (Prom2)	chr11:95,643,795-95,644,453	659

[a]Coordinates are from the February 2009 UCSC Human Genome Browser (hg19).

alternative first exon; Figure 2A). Importantly, this region does not map to any annotated exons for *MTMR2*, including the previously reported, alternatively spliced exons at the 5' end of the locus (9,27). We also scrutinized RNA-seq data generated using five unique passages of S16 cells (Law and Antonellis, manuscript in preparation). This revealed abundant reads that map to either the annotated exon 1 or the newly identified exon just downstream of MCS3. An average of 124 reads per sample map to exon 1 (S.D. ± 21) including an average of 32 split reads to exon 2 (S.D. ± 9). An average of 60 reads per sample map to the region downstream of MCS3 (S.D. ± 33) including an average of 11 split reads to exon 2 (S.D. ± 7). Moreover, no split reads mapped to the 5' end of the newly identified exon, indicating that this is a transcription start site, and not an alternatively spliced exon; these findings are consistent with the above 5'-RACE data. Combined, our findings indicate that *MTMR2*-MCS3 represents a previously unreported alternative promoter that directs expression of a newly identified first exon at *MTMR2*. Therefore, we renamed this regulatory element *MTMR2*-Prom2 and the adjacent transcribed region *MTMR2* exon 1B.

The MTMR2-2 mRNA is expressed in Schwann cells

To define the expression of *MTMR2* transcripts with respect to the associated CMT phenotype, we performed first-exon-specific RT-PCR on cDNA samples from cells relevant to the peripheral nervous system and CMT disease: mouse sciatic nerve (mSN), MN-1 cells, and immortalized mouse muscle cells (C2C12) (28). Importantly, the majority of mRNA from sciatic nerve is from Schwann cells, which provides information about Schwann cell gene expression *in vivo*. While all of the tested cells express exon 1A-containing *Mtmr2* transcripts, only sciatic nerve expresses *Mtmr2* exon 1B-containing transcripts (Figure 2B); note that the original detection of transcripts harbouring exon 1B was performed on cDNA from immortalized rat Schwann (S16) cells (see above and Figure 2A). In addition, we routinely detected multiple bands in *Mtmr2* RT-PCR products, reflecting mRNA isoforms produced by the alternative inclusion of multiple 'second exons'; this was confirmed by sequencing each PCR product (data not shown).

The above findings raised the question of whether the two *Mtmr2* isoforms, both expressed in Schwann cells *in vivo*, are differentially expressed during development (*i.e.* myelination). To determine the relative levels of the exon 1A- and 1B-containing transcripts *in vivo*, we compared the two isoforms in rat sciatic nerve to the levels found in S16 cells (both transcripts are expressed at similar levels in these cells, see below) via quantitative RT-PCR experiments on sciatic nerve samples from P1 and P15 rats with first-exon specific primers. After normalization to 18S rRNA, the ratio of exon 1A transcript *in vivo* to that found in S16 cells was approximately 1 in both P1 and P15 sciatic nerve. In contrast, the exon 1B transcript was ~5-fold elevated in the sciatic nerve samples compared to S16 cells, at both P1 and P15. Therefore, the exon 1B isoform is expressed *in vivo* at least at the same level as, or even higher than, the exon 1A transcript (Figure 2C). However, while *Mtmr2* is developmentally regulated (12), this does not appear to be due to an increase in either transcript, which makes *Mtmr2* similar to *Pmp22* (29).

To ensure that exon 1B-containing transcripts represent a full-length *MTMR2* mRNA, we performed long-range RT-PCR on cDNA isolated from S16 cells with a forward primer designed in *Mtmr2* exon 1B and a reverse primer designed in the last coding exon of *Mtmr2*. This revealed a single PCR product of the expected size of 1.8 kilobases (Figure 2D). We then cloned the above PCR product and subjected it to DNA sequence analysis, which revealed the presence of all protein-coding exons downstream of exon 1B (Figure 2A); we were also able to amplify and sequence-verify a full-length cDNA initiated from exon 1A in S16 cells (data not shown), which we used for protein localization studies (see below). To investigate whether this full transcript is expressed in Schwann cells *in vivo*, we repeated the long-range RT-PCR with cDNA isolated from mouse sciatic nerve and primers specific to mouse *Mtmr2* exon 1B and the last coding exon. Similarly, this generated a single PCR product (Figure 2E) that was subject to DNA sequence analysis, again revealing the presence of all protein-coding exons. These data confirmed that the *MTMR2*-2 mRNA is expressed in Schwann cells *in vivo* and encodes a shorter, N-terminally truncated protein isoform (see below and Figure 3).

MTMR2 transcripts initiated from exon 1B (Figure 3A) are predicted to encode a shorter protein isoform (MTMR2-2), which lacks the first 72 amino acids at the N-terminus (Figure 3B). This protein isoform has been noted in the literature previously (9) and was proposed to originate from exon 1A-containing transcripts when an alternatively spliced exon that contains a stop codon (exon 2A) is included (27). Importantly, the N-terminally truncated MTMR2-2 isoform retains all of the known functional domains of the protein, but lacks a phosphorylation site (serine 58; S58 in Figure 3B) proposed to regulate the localization of MTMR2-1 to endosomes (30). Considering the enrichment of exon 1B-containing transcripts in sciatic nerve compared to cultured motor neurons (Figure 2B), it is possible that there is also an enrichment of MTMR2-2 proteins in Schwann cells relative to motor neurons. Unfortunately, due to our inability to acquire a specific antibody against endogenous MTMR2, we were unable to address this possibility (Supplementary Figure 1A–C). However, our data show that the *MTMR2*-Prom2 is active in Schwann cells and directs the expression of an alternative *MTMR2* mRNA (*MTMR2-2*; Figure 3A) that is predicted to encode for the MTMR2-2 protein isoform (Figure 3B).

SOX10 regulates MTMR2-Prom2 activity in Schwann cells

SOX10 is an important regulator of gene expression in Schwann cells and many SOX10 target genes are known to be important for Schwann cell function. To investigate if SOX10 plays a role in the activity of *MTMR2*-Prom2 in Schwann cells, we analysed this region for evidence of SOX10 binding *in vivo* using a previously published data set. ChIP-seq analyses from rat sciatic nerve, which is enriched for Schwann cell nuclei, contained evidence of SOX10 binding at this promoter (Figure 4A), indicating that SOX10 binds to this element *in vivo* (31). Furthermore, this region is recognized by an antibody against H3K27Ac (31), which marks active regulatory elements, and by an antibody against H3K4me3, indicative of an active promoter element (Figure 4A). These findings led us to analyse this region for binding by EGR2/KROX20, which is a transcription factor that works synergistically with SOX10 at adjacent binding sites to regulate gene

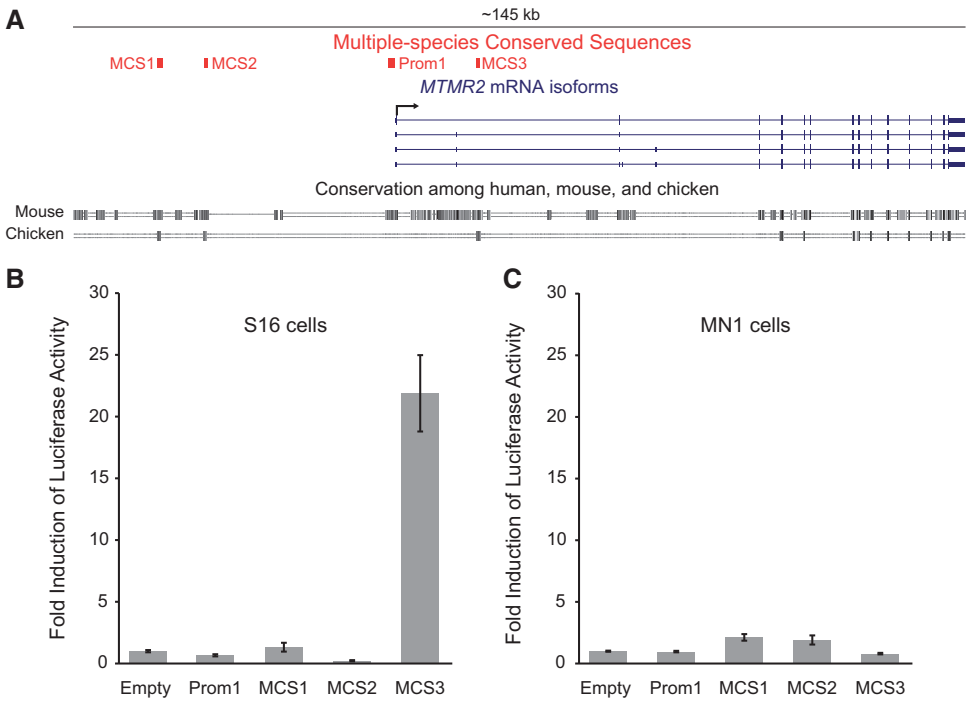

Figure 1. *MTMR2*-MCS3 is an active regulatory element in immortalized rat Schwann cells. (**A**) The ~145 kb *MTMR2* locus was analysed for non-coding regions conserved between human, mouse, and chicken genomes (indicated along the bottom in black). The locations of the three multiple-species conserved sequences (MCS1-3) and the proximal promoter (Prom1) are indicated in red along with the four described *MTMR2* mRNA isoforms (indicated in blue, see text for details), which are transcribed from left to right (black arrow). (**B and C**) The four elements identified in (A) were cloned upstream of a luciferase reporter gene and tested for induction of luciferase activity in S16 cells (B) and MN-1 cells (C) relative to an 'empty' control vector with no genomic insert. Error bars indicate standard deviation.

expression during myelination (32,33). This did not reveal any evidence of EGR2/KROX20 binding within the alternative promoter or anywhere else at *MTMR2* (data not shown). In summary, our data support the conclusion that *MTMR2*-Prom2 is an active promoter that is bound by SOX10 in rat sciatic nerve.

SOX10 binds to a well-characterized consensus sequence (34) as a monomer or as a dimer when two consensus sequences are arranged in a head-to-head fashion (35). We therefore visually examined the *MTMR2*-Prom2 element for conserved SOX10 consensus sequences, which revealed a dimeric SOX10 consensus site that is conserved between human and chicken (Figure 4B; note that 'ACAAT' is also a highly confident SOX10 consensus sequence). To determine if the dimeric consensus sequence is important for the regulatory activity of *MTMR2*-Prom2 in Schwann cells, we generated a luciferase reporter construct containing *MTMR2*-Prom2 with the dimeric SOX10 consensus sites and the intervening sequences deleted (ΔSOX10). When this construct was transfected into S16 cells, the regulatory activity was reduced by ~90% compared to wild-type *MTMR2*-Prom2 (Figure 4C), indicating that the dimeric SOX10 consensus sequence is critical for the full activity of the alternative promoter.

To determine the sufficiency of SOX10 in activating *MTMR2*-Prom2, wild-type and ΔSOX10 *MTMR2*-Prom2 constructs were transfected into MN-1 cells, which lack endogenous SOX10 (24). In agreement with earlier results (Figure 1C), both reporter constructs show very little regulatory activity in MN-1 cells (Figure 4D). However, upon overexpression of exogenous SOX10 in these cells, *MTMR2*-Prom2 directs luciferase expression ~100-fold higher than *MTMR2*-Prom2 in the absence of SOX10 (Figure 4D). Furthermore, deletion of the dimeric SOX10 binding site reduces the responsiveness to SOX10 by ~60% (Figure 4D). Notably, the *MTMR2*-Prom2 element contains other conserved and non-conserved SOX10 consensus sequences (Supplementary Material, Fig. 2A), which may explain the remaining 40% of activity associated with ΔSOX10 *MTMR2*-Prom2 upon overexpression of SOX10 in MN-1 cells. We also found that *MTMR2*-Prom2 can be stimulated by expression of SOX8 and SOX9, which bind to similar sequences as SOX10 (36); however, SOX10 has the largest effect on regulatory activity (Supplementary Material, Fig. 2B). Upon examining *MTMR2*-Prom2 at the UCSC Human Genome Browser, we identified two annotated SNPs within *MTMR2*-Prom2; however, neither reside within the dimeric SOX10 binding site and neither affect the regulatory activity of *MTMR2*-Prom2 (data not shown). Combined, these data indicate that SOX10 is sufficient to activate *MTMR2*-Prom2 in MN-1 cells.

To investigate the necessity of SOX10 for *MTMR2*-Prom2 activity in Schwann cells, wild-type and ΔSOX10 Prom2 were each transfected into S16 cells along with a construct to express dominant-negative (E189X) SOX10, which interferes with the function of endogenous SOX10 (37). The levels of luciferase induction from each construct alone were consistent with our previous experiments (Figure 4C and E). In contrast, expression of the dominant-negative SOX10 protein nearly ablates the regulatory activity of wild-type *MTMR2*-Prom2 (Figure 4E). These data indicate that SOX10 is necessary for the activity of this element in Schwann cells.

SOX10 is required for expression of endogenous MTMR2 transcripts harbouring exon 1B

Based on our findings that exon 1B-containing transcripts are not expressed in MN-1 cells (Figure 2B) and that overexpression of SOX10 induces the activity of *MTMR2*-Prom2 in MN-1 cells (Figure 3D), we tested if SOX10 is sufficient to induce the

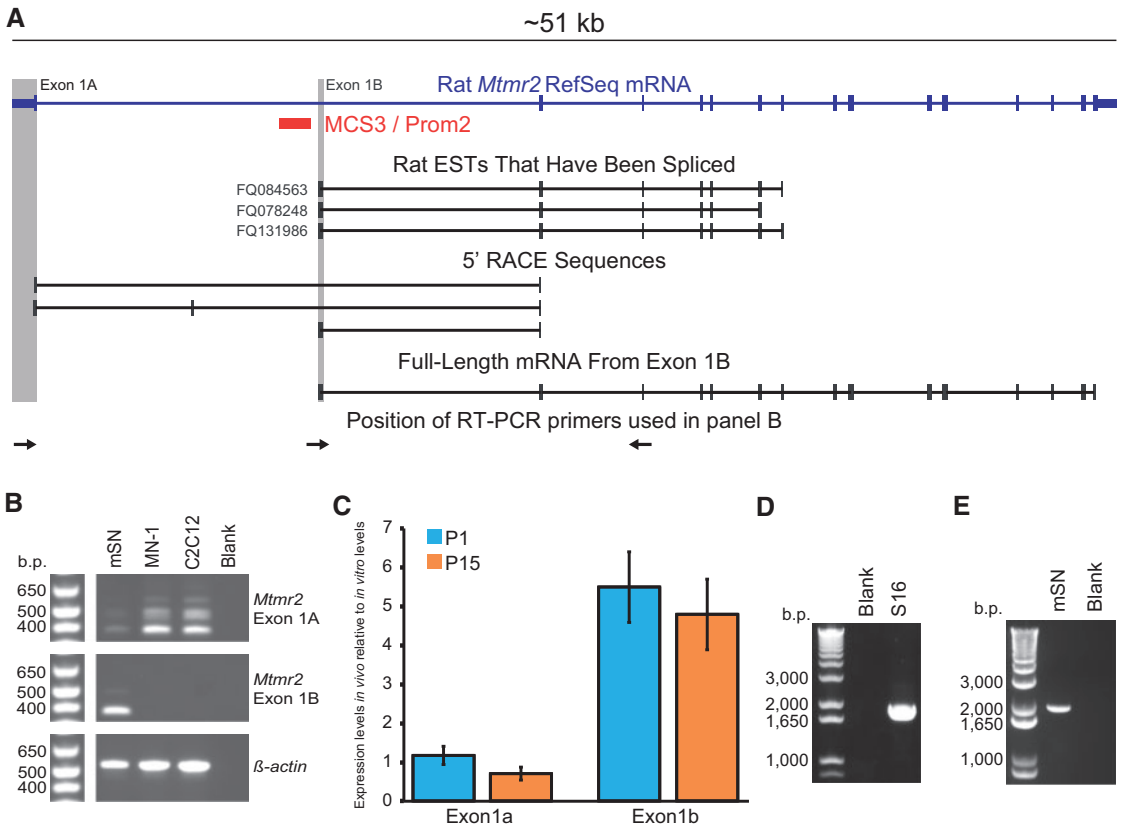

Figure 2. *MTMR2*-MCS3 is an alternative promoter that is active in Schwann cells. (**A**) The ~51 kb rat *Mtmr2* transcriptional unit (indicated in blue) from the UCSC Genome Browser is shown along with MCS3 (red), rat expressed sequence tags (ESTs), three distinct *Mtmr2* mRNA 5' ends identified by 5' RACE, and the full-length *Mtmr2* mRNA generated from exon 1B. The grey shading indicates the position of exons 1A and 1B. (**B**) RT-PCR assay to test for the presence of exon 1A- and exon 1B-containing transcripts in mouse sciatic nerve (mSN), immortalized motor neurons (MN-1), and immortalized muscle cells (C2C12). Negative controls without cDNA (Blank) were included for each primer pair and primers for *β-actin* were used as a positive control. Base pair (b.p.) sizes of markers are provided on the left. (**C**) Quantitative RT-PCR was performed to determine the expression levels of exon 1A- and 1B-containing *Mtmr2* transcripts in P1 and P15 rat sciatic nerve relative to the levels in the S16 Schwann cell line, after normalization to 18S rRNA. Average and standard deviations are shown for three biological replicates. (**D**) A full-length mRNA was amplified from Schwann (S16) cell cDNA using long-range RT-PCR and primers designed in exon 1B and in the last coding exon of *Mtmr2*. A negative control without cDNA was included (Blank). (**E**) A full-length mRNA was amplified from mouse sciatic nerve cDNA using long-range RT-PCR and primers designed in exon 1B and in the last coding exon of *Mtmr2*. A negative control without cDNA was included (Blank).

expression of endogenous exon 1B-containing transcripts in these same cells. MN-1 cells were transfected with constructs to express SOX10 or dominant-negative (E189X) SOX10, or were mock transfected in the absence of a SOX10 expression construct. Remarkably, exon-specific RT-PCR assays showed that the expression of exogenous SOX10 is sufficient to induce endogenous *Mtmr2-2* mRNA expression in cultured MN-1 cells (Figure 4F; the specificity of PCR products was confirmed by DNA sequence analysis, not shown).

To assess the requirement of SOX10 for the expression of each *MTMR2* transcript (*MTMR2-1* vs. *MTMR2-2*), we performed siRNA knockdown of SOX10 in S16 cells and in cultured primary rat Schwann cells. The expression levels of endogenous rat *Mtmr2* exon 1A- and exon 1B-containing transcripts were measured using quantitative RT-PCR and primers specific to each first exon. In S16 cells, exon 1A-containing transcripts were ~40% reduced with SOX10 knockdown compared to control siRNA. However, exon 1B-containing transcripts were almost completely eliminated with SOX10 knockdown (Figure 4G). These analyses also indicate that exon 1A- and 1B-containing transcripts are expressed at approximately equal levels in S16 cells; exon1B transcripts are virtually absent in siSox10-treated S16 cells (Figure 4G) whereas total *Mtmr2* levels are reduced ~50% in siSox10-treated S16 cells (data not shown). Similarly, in primary rat Schwann cells, exon 1A-containing transcripts were not significantly affected by SOX10 knockdown, while exon 1B-containing transcripts show near-complete abolishment (Figure 4H). Taken together, our data indicate that SOX10 is necessary and sufficient for the expression of *Mtmr2-2*.

Overexpressed MTMR2 protein isoforms differentially localize to the nucleus in cultured cells

Our data suggest an important role of the shorter MTMR2 protein isoform (MTMR2-2) in Schwann cells. To investigate the functional differences between the two MTMR2 protein isoforms, we transiently transfected HeLa cells with constructs to express each isoform with an N-terminal GFP tag and performed fluorescence microscopy. We found that both proteins localize diffusely in the cytoplasm as well as to discrete puncta, and that these puncta are more clearly visualized upon treating the cells with saponin to deplete cytosolic proteins (Figure 5A). Interestingly, cells expressing GFP-MTMR2-2 exhibited puncta more frequently than those expressing GFP-MTMR2-1 (Figure 5B). Approximately 20% of GFP-positive cells expressing GFP-MTMR2-1 have at least five distinct cellular puncta. In contrast, ~75% of cells expressing GFP-MTMR2-2 met this criteria

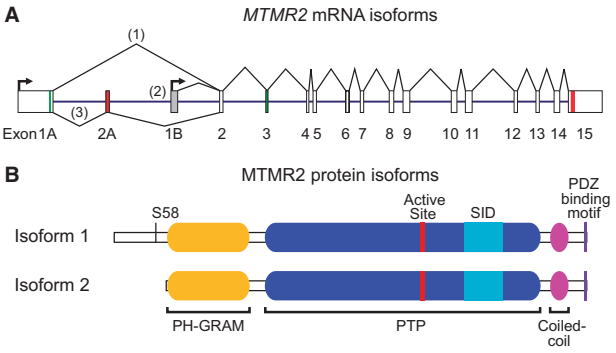

Figure 3. A new model of transcriptional activity at the *MTMR2* locus. (**A**) Schematic of the *MTMR2* locus including transcription start sites (arrows), translation start codons (green), and stop codons (red). Exon numbers are provided along the bottom. Multiple mRNA isoforms (*MTMR2-1*, *MTMR2-2*, and *MTMR2-3*) are produced via alternative splicing and alternative promoter use. (**B**) MTMR2 protein isoforms are shown indicating the pleckstrin homology/glucosyltransferases, Rab-like GTPase activators, and myotubularins (PH-GRAM; yellow), protein tyrosine phosphatase (PTP; blue), active site (red), SET interaction (SID; aqua), coiled coil (magenta), and PSD-95, Discs-large, ZO-1 binding (PDZ; purple) domains. Please note that isoform 2 lacks 72 amino acids at the N terminus, including the phosphorylation site Serine 58 (S58).

(GFP-MTMR2-1 $n = 542$, GFP-MTMR2-2 $n = 554$, test for two-sample proportions, $z = 18.709$, $P < 0.0001$).

Our fluorescence microscopy analyses also revealed that the MTMR2 puncta frequently overlap with nuclear DAPI staining (Figure 5A). To assess for nuclear localization of MTMR2 protein isoforms, we isolated cytosolic and nuclear protein fractions from cells transiently transfected with constructs to express GFP-MTMR2-1 or GFP-MTMR2-2. We found that both MTMR2 isoforms localize to the cytosolic and nuclear fractions, but that a larger fraction of GFP-MTMR2-2 is present in the nucleus compared to GFP-MTMR2-1 (Figure 5C). To confirm that the MTMR2 puncta are nuclear, we performed confocal fluorescent microscopy on HeLa cells expressing either GFP-MTMR2-1 or GFP-MTMR2-2. This revealed that both MTMR2 isoforms localize to nuclear puncta (Figure 5D), again with a larger percentage identified in cells expressing GFP-MTMR2-2. The perinuclear localization of some MTMR2 puncta raised the question of whether these proteins localize to the endoplasmic reticulum (ER). To assess this possibility, we visualized the ER in GFP-MTMR2-transfected HeLa cells with an antibody against the ER resident protein Calnexin, and found no consistent indications of co-localization (Supplementary Material, Fig. 3). To rule out a GFP-specific effect in localization, the above protein studies were repeated with constructs expressing N-terminally Flag-tagged MTMR2 protein isoforms, with results completely consistent with GFP-tagged proteins (Supplementary Material, Fig. 4). As mentioned above, the lack of a specific MTMR2 antibody precluded us from determining the nuclear localization of either endogenous protein isoform *in vitro* or *in vivo*. Taken together, our data suggest that MTMR2 has a nuclear function; indeed, MTMR2 has been previously reported to localize to the nucleus (18).

Discussion

Loss-of-function mutations in *MTMR2* cause autosomal recessive CMT4B1, a Schwann cell-specific demyelinating peripheral neuropathy; however, *MTMR2* is a ubiquitously expressed gene (38). To investigate this discrepancy and clarify any specific role of MTMR2 in Schwann cells, we used evolutionary conservation to identify candidate transcriptional regulatory elements at *MTMR2*. These studies identified an alternative *MTMR2* promoter that is active in immortalized Schwann cells and that mediates the expression of a novel mRNA transcript; this mRNA is enriched in Schwann cells compared to motor neurons. Closer analysis of the promoter element revealed a predicted dimeric SOX10 binding site that is evolutionarily conserved. SOX10 is essential for long-term Schwann cell function and directly regulates many genes important for myelination in the peripheral nerve (36,39). Our functional studies revealed that the SOX10 consensus sequence is responsible for a large portion of the regulatory activity of this alternative promoter. Furthermore, we showed that the regulatory activity and the generation of the associated mRNA transcript are reduced with disruption of SOX10 function in Schwann cells and induced with the expression of exogenous SOX10 in motor neurons. These data indicate that SOX10 is both necessary and sufficient for the activity of a Schwann cell promoter at *MTMR2* that directs the expression of a previously unreported transcript. Interestingly, we found that the *Mtmr2* isoforms are not differentially expressed across the postnatal myelination period in rat sciatic nerves. However, as SOX10 is expressed throughout the Schwann cell lineage, beginning in migrating neural crest cells and persisting in the mature myelinating Schwann cell, we cannot rule out differential expression at other stages in Schwann cell development.

Mutations in non-coding transcriptional regulatory sequences can cause or modify human disease and the identification of regulatory elements at disease-associated loci increases the genomic space to screen for disease-associated mutations. Indeed, CMT-associated loci have been shown to harbour non-coding mutations that cause or modify CMT disease, including *GJB1*and *SH3TC2* (40–42). Because CMT4B1 is a recessive disease caused by loss-of-function *MTMR2* mutations, we predict that patients with a CMT4B1 phenotype but who do not carry *MTMR2* protein-coding mutations (or who carry only one coding mutation) may carry non-coding mutations at this locus. Regulatory elements important for *MTMR2* expression, including the alternative promoter reported here, are excellent candidate regions for disease-causing mutations.

The findings presented here support a new model of transcriptional regulation at the *MTMR2* locus, with at least three mRNA products produced from two promoters (Figure 3A), which allow variable expression of two protein isoforms (Figure 3B). The first (*MTMR2-1*) and third (*MTMR2-3*) transcripts are expressed from *MTMR2*-Prom1 and include exon 1A. *MTMR2-1* excludes exon 2A, which harbours an in-frame stop codon and results in expression of the full-length MTMR2-1 protein. *MTMR2-3* includes the stop codon in exon 2A, which results in the expression of the N-terminally truncated MTMR2-2 protein isoform. Finally, the novel mRNA described here (*MTMR2-2*) is generated from *MTMR2*-Prom2, includes exon 1B, and only encodes the shorter protein isoform MTMR2-2.

Our transcriptional regulatory data suggest that the MTMR2-2 protein plays an important role in Schwann cells. To investigate this possibility, we analysed the localization of each protein isoform when overexpressed in HeLa cells. These studies revealed that both isoforms localize both diffusely in the cytoplasm and to discrete puncta. However, MTMR2-2 shows a greater propensity toward puncta formation than MTMR2-1. Furthermore, we found that each isoform localizes to puncta within the cell nucleus, and that MTMR2-2 shows greater nuclear localization compared to MTMR2-1. While these findings

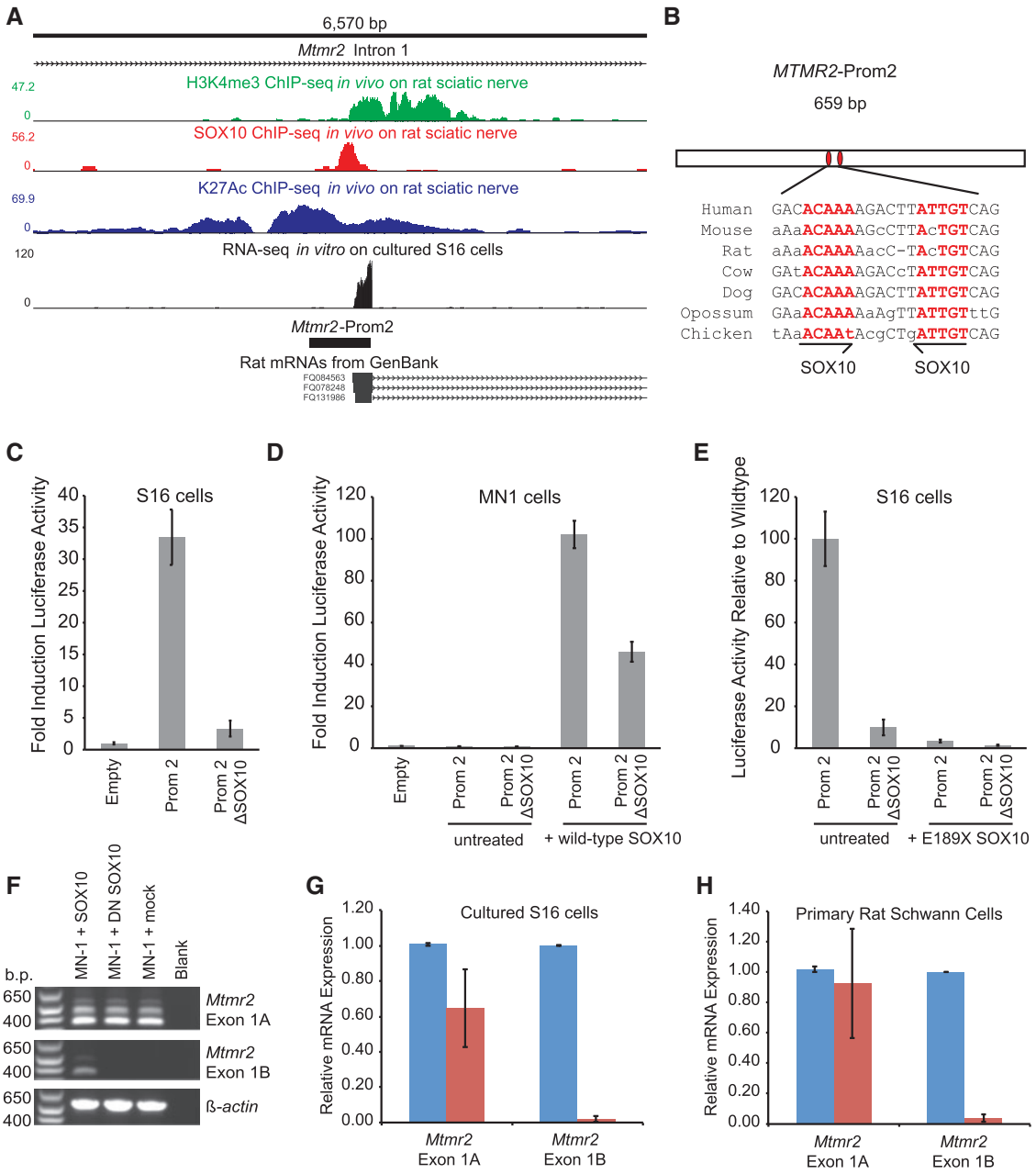

Figure 4. SOX10 regulates the activity of *MTMR2*-Prom2 and the expression of the *MTMR2*-2 mRNA. (**A**) A ~6.6 kb region of *MTMR2* intron 1 is shown along with ChIP-Seq data for histone 3 lysine 4 trimethylation (H3K4me3; green), SOX10 (red), and histone 3 lysine 27 acetylation (H3K27Ac; blue) all performed on rat sciatic nerve. RNA-Sequencing reads, showing per-base read depth across 2 samples of S16 cells, *MTMR2*-Prom2, and spliced rat *MTMR2* ESTs are also indicated. (**B**) The 659 base pair *MTMR2*-Prom2 is shown along with the position of the two SOX10 monomeric consensus sequences (red ovals and red text). The seven species utilized for comparative sequence analysis are shown on the left, with lower-case letters indicating bases not conserved among all seven species. Half arrows indicate the position and orientation of the two monomeric SOX10 consensus sequences. (**C**) *MTMR2*-Prom2 with or without (ΔSOX10) the dimeric SOX10 sequence was cloned upstream of a luciferase reporter gene, transfected into cultured Schwann (S16) cells, and tested for activity in luciferase assays compared to an empty vector containing no genomic insert. The fold induction of luciferase activity is indicated along the y axis and error bars indicate standard deviations. (**D**) Wild-type and ΔSOX10 *MTMR2*-Prom2 were evaluated for regulatory activity in MN1 cells using luciferase assays as in (C) in the presence and absence of a construct to express SOX10. (**E**) Wild-type and ΔSOX10 *MTMR2*-Prom2 were evaluated for regulatory activity in S16 cells using luciferase assays as in (C) in the presence and absence of a construct to express dominant-negative (E189X) SOX10. (**F**) RT-PCR assays were performed as in Figure 2B using cDNA prepared from MN-1 cells transfected with a construct to express either wild-type or dominant-negative SOX10, or mock transfected without a SOX10 expression construct. Note that transfection of the wild-type SOX10 expression construct was sufficient to allow detection of endogenous *Mtmr2* exon 1B-harbouring transcripts. (**G and H**) S16 cells and rat Schwann cells were treated with siRNA targeted against SOX10 (red) or control siRNA (blue). Quantitative RT-PCR was used to measure expression levels of *Mtmr2* exon 1A- and exon 1B-containing transcripts. Error bars indicate standard deviations.

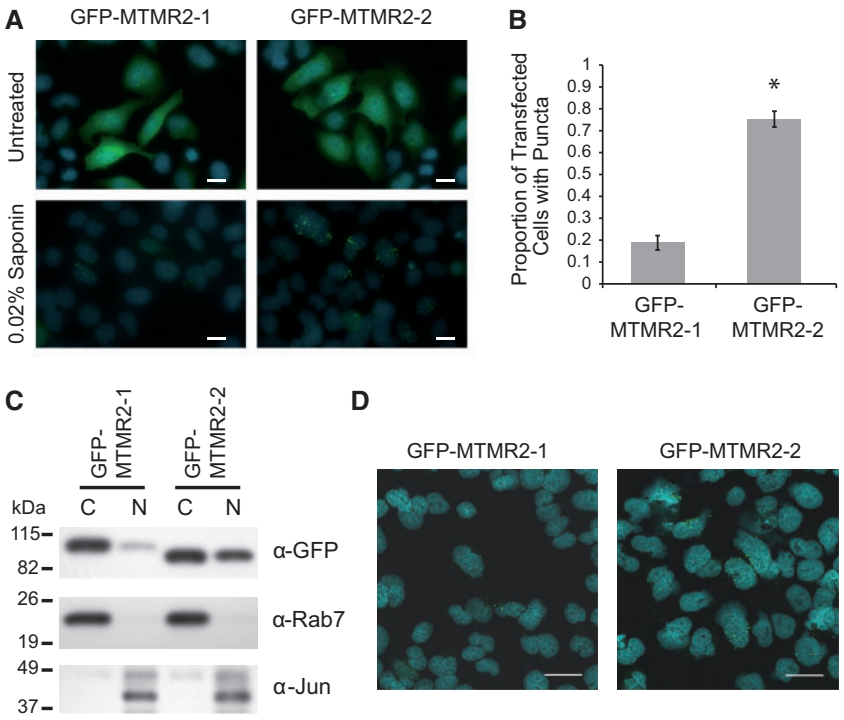

Figure 5. MTMR2 protein isoforms differentially localize to subcellular puncta and to the cell nucleus. (**A**) HeLa cells were transfected with constructs to express GFP-MTMR2 isoforms and imaged with standard fluorescence microscopy. Cells were untreated or treated with 0.02% saponin to remove cytosolic proteins and stained with DAPI to visualize nuclei prior to fixation. Scale bars, 20 μm. (**B**) Quantification of puncta formed by the two MTMR2 isoforms. Statistical analysis: significance test for two-sample proportions (MTMR2-1 $n = 542$, MTMR2-2 $n = 554$, $P < 0.0001$). Error bars represent margin of error for 95% confidence interval. (**C**) Western blot using an anti-GFP antibody and 20 μg of cytosolic (C) or nuclear protein (N) fractions isolated from HeLa cells transfected with constructs to express either GFP-MTMR2 isoform 1 or isoform 2. Rab7 and cJun antibodies were used on the same blot to assess protein loading and fraction purity. A protein marker in kilodaltons (kDa) is indicated on the left. (D) HeLa cells were transfected with constructs to express either GFP-MTMR2 isoform, treated with 0.02% saponin to clear cytosolic proteins and DAPI to visualize nuclei (blue), and imaged with a confocal fluorescence microscope. Each image was taken from a single 0.3 μm-depth slice in the z-stack. Scale bars, 30 μm.

support the notion that there are physiological differences between the two protein isoforms and provide evidence for a nuclear function of MTMR2, further studies on the function of MTMR2 isoforms in Schwann cells *in vivo* are required (*e.g.* developing isoform-specific antibodies and generating mouse models with targeted disruptions of each MTMR2 isoform in isolation).

The studies described here reveal strong evidence for a previously unappreciated transcriptional regulation mechanism at *MTMR2* in Schwann cells. Our findings provide a better understanding of the biology of the *MTMR2* locus, increase the mutational screening space for patients with CMT4B1, and raise questions about the global use of alternative promoters in the development and function of glial cells (24,29,43,44).

Materials and Methods

Comparative sequence analysis at MTMR2

To identify non-coding multiple species conserved sequences (MCSs) at *MTMR2* we scrutinized the human *MTMR* locus on chromosome 11 including genomic sequences up to the two flanking genes using the UCSC Human Genome Browser (21): *CEP57* (centromeric) and *MAML2* (telomeric). This resulted in the assessment of a 143,901 base pair genomic region (chr11:95,565,857-95,709,757; hg19). Next, we visually examined the 'Multiz Alignments of 100 Vertebrates' track (21) for non-coding genomic sequences that aligned between human, mouse, and chicken – three vertebrate species relevant for the study of peripheral nervous system myelination. These efforts revealed three regions of interest (MSC1, MCS2, and MCS3; Table 1 and Figure 1A); however, we also included the *MTMR2* proximal promoter (Table 1 and Figure 1A) in our functional studies.

Generation of reporter gene and expression constructs

Oligonucleotide primers containing attB1 and attB2 Gateway cloning sequences (Invitrogen Life Technologies, Carlsbad, CA) were designed for PCR-based amplification of the *MTMR2* Promoter and each MCS (Table 1) and of the two *Mtmr2* open reading frames (ORFs; all primer sequences available upon request). Putative regulatory sequences were amplified from human genomic DNA and the *Mtmr2* ORFs were amplified from a cDNA library generated from RNA extracted from rat S16 cells (see below) using Phusion High-Fidelity DNA Polymerase (New England Biolabs Inc., Ipswich, MA). Subsequent to PCR amplification and purification, each genomic segment was cloned into the pDONR221 vector using BP Clonase (Invitrogen). Resulting constructs were genotyped by digestion with *Bsr*GI and subjected to DNA sequence analysis to ensure the integrity of the insert. For luciferase assays, each resulting pDONR221 construct was recombined with an expression construct (pE1B-luciferase) (25) using LR Clonase (Invitrogen) to clone each region upstream of a minimal promoter directing expression of a luciferase reporter gene. For localization studies, each resulting pDONR221 construct was recombined with an expression construct using LR Clonase to clone each ORF in frame with an N-terminal GFP (pcDNA-pDEST53, Invitrogen) or Flag tag [pEZYflag, Addgene

plasmid #18700 (45)]. In each case, successful recombination was confirmed via digestion of DNA with *Bsr*G1 (New England Biolabs Inc.). DNA sequencing analysis was employed to confirm that the ORFs were in-frame with the tag.

Site-directed mutagenesis was performed using the QuikChange II XL Site-Directed Mutagenesis Kit (Agilent Technologies, Inc., Santa Clara, CA). Mutagenesis primers (available upon request) were designed to delete the dimeric SOX10 binding site within *MTMR2*-Prom2 and produce the minor alleles of the two SNPs identified in *MTMR2*-Prom2. Mutagenesis was performed in pDONR221 constructs (see above) and DNA from each resulting clone underwent sequence analysis to verify that only the desired mutation was produced. Verified clones were then recombined into pE1B-luciferase using LR Clonase (Invitrogen).

Cell culture, transfection and luciferase assays

Immortalized rat Schwann cells (S16) (22), mouse spinal motor neurons (MN-1) (26), and HeLa cells were grown under standard conditions in DMEM with 10% fetal bovine serum, 2mM L-glutamine, 50 U/ml penicillin, and 50 g/ ml streptomycin. For luciferase assays, $\sim 1\times10^4$ S16 or MN-1 cells were plated in each well of a 96-well plate. For RT-PCR and Western blot experiments, $\sim 3.5\times10^5$ S16, MN-1, C2C12, or HeLa cells were plated in each well of a 6-well plate. For localization studies, $\sim 5\times10^4$ HeLa cells were plated in each chamber of a 4-chamber slide. For all experiments, cells were cultured for 24 h under standard conditions prior to transfections.

Lipofectamine 2000 (Life Technologies) was diluted 1:100 in OptiMEM I reduced serum medium (Life Technologies) and incubated at room temperature for 10 min. Each DNA construct to be transfected was individually diluted in OptiMEM to a concentration of 8 ng/μl (96-well plates), 4 ng/μl (6-well plates), or 12 ng/μl (4-chamber slides). For luciferase assays, an internal control renilla construct was added to the solution at 8 pg/μl. For co-expression in luciferase assays, 100 ng of a construct to express either wild-type or dominant-negative (E189X) SOX10 (37) was co-transfected in each well. One volume of lipofectamine solution was added to each DNA solution and allowed to sit for 20 min at room temperature. Cells were incubated with transfection solution for 4 h under standard conditions and then the media was changed to standard growth medium.

For luciferase assays, S16 or MN-1 cells were washed with 1X PBS 48 h after transfection and lysed for 1 h shaking at room temperature using 1X Passive Lysis Buffer (Promega, Madison, WI). 10 μl of lysate from each well was transferred into a white polystyrene 96-well plate (Corning Inc., Corning, NY). Luciferase and renilla activities were determined using the Dual Luciferase Reporter 1000 Assay System (Promega) and a Glomax Multi-Detection System (Promega). Each reaction was performed at least 24 times. The ratio of luciferase to renilla activity and the fold change in this ratio compared to a control luciferase expression vector with no genomic insert were calculated. The mean (bar height) and standard deviation (error bars) of the fold difference are represented in the figures.

Fluorescence microscopy

For localization studies, cells were cultured under standard conditions for 24 h after transfection. Cells were then washed with 1X PBS for 5 min, fixed with 4% paraformaldehyde in PBS for 10 min at room temperature, washed 3 times with PBS, permeabolized with 0.1% Triton X-100 in PBS for 10 min at room temperature, and washed 3 times again with PBS. Cells were blocked with 1% BSA in PBS for 2 h, shaking at room temperature. To enhance GFP signal, GFP-MTMR2-transfected cells were incubated for 1.5 h at 37 °C with a monoclonal mouse GFP antibody (Clone 3E6, Invitrogen) diluted 1:200 in 1% BSA. Similarly, Flag-MTMR2-transfected cells were incubated under the same conditions with a monoclonal mouse Flag antibody (Clone M2, Sigma) diluted 1:2000. For colocalization experiments with Calnexin, transfected cells were incubated with a rabbit GFP antibody conjugated to AlexaFluor 488 (Invitrogen) diluted 1:1000 and a monoclonal mouse Calnexin antibody (EMD Millipore, C8.B6) diluted 1:250. After washing, cells were incubated for 1 h at 37 °C with AlexaFluor 488 or 555 goat anti-mouse secondary antibody (Invitrogen) diluted 1:1000 in 1% BSA. All cells were stained with DAPI to visualize nuclei. ProLong Gold anti-fade reagent (Invitrogen) was applied and slides were covered with glass coverslips. For saponin treatment, cells were incubated in 0.02% saponin (Sigma-Aldrich, St. Louis, MO) in 1X PBS for 2 min at room temperature, then washed three times with PBS prior to fixation. For standard fluorescent microscopy, cells were imaged with an Olympus IX71 inverted microscope using cellSens Standard image software (Olympus, Center Valley, PA). For confocal fluorescent microscopy, cells were imaged with a Leica Upright SP5X Confocal Microscope or a Nikon A-1 Confocal Microscope in the University of Michigan Microscopy & Image Analysis Core Laboratory. Cell counts to quantify puncta formation were done across three independent transfections, and were confirmed by additional counts from an observer naïve to the nature of the experiments.

RNA isolation, cDNA library preparation, and 5'RACE

RNA was isolated from S16, MN1, C2C12, or HeLa cells (immediately or 24 h after transfection) or from fresh mouse sciatic nerve or whole brain from animals of either sex using the RNeasy Mini Kit (Qiagen, Vinlo, Limburg) according to manufacturer's instructions, eluted into 50 μl of RNase-free water, and stored at −80 °C. RNA concentration and purity were determined using a NanoDrop Lite (Thermo Scientific, Waltham, MA). A cDNA library was generated from each sample using 1 μg of RNA and the high-capacity cDNA reverse transcription kit (Life Technologies), with the provided random reverse-transcription primers.

For 5'RACE experiments, first-strand cDNA was generated from RNA isolated from S16 cells using an oligonucleotide primer designed in exon 5 of the rat *Mtmr2* locus. The cDNA sample was subsequently TdT-tailed using the 5'RACE System (Invitrogen) and sequential PCR reactions were performed using nested primers in exon 4 and exon 2 of *Mtmr2*. PCR products were size separated by gel electrophoresis, excised, purified using the QIAquick Gel Extraction Kit (Qiagen, Venlo, Netherlands), and subjected to TA cloning. A total of 28 DNA samples extracted from individual clones were subjected to DNA sequence analysis, 19 of which mapped to the rat *Mtmr2* locus.

RT-PCR

cDNA samples were analysed by PCR using species- and gene-specific primers. For studies in rat we used the following primers: Exon 1A_RT_F, 5'-ATGGAGAAGAGCTCGAGCTG-3"; Exon 1B_RT_R, 5'-AAGCAAGTGGTTTAGATCTCACTGT-3'; and RT_R, 5'-TTGATGTTCTCTCCTGGAAGC-3' (mouse primer sequences available upon request). For each reaction, 23 μl of PCR Supermix (Life

Technologies) was combined with 0.5 μl of each 20 μM primer solution and 1 μl of cDNA. Reactions to amplify the full-length *Mtmr2-2* transcript from S16 cells and mouse sciatic nerve were done with phusion high-fidelity polymerase (NEB). Blank (cDNA-negative) controls were included for each primer pair. Standard PCR conditions were used.

Western blot analysis

Cytosolic and nuclear protein fractions were isolated using the NE-PER kit (Thermo Scientific) according to the manufacturer's instructions. For sciatic nerve lysates, nerves were sonicated in 200 μl of lysis solution containing 25 mM Tris-HCl/150mM NaCl/1% NP-40/1% sodium deoxycholate/0.1% SDS (Thermo Scientific) and protease inhibitor cocktail (Thermo Scientific). Protein concentrations were quantified using the BCA Protein Assay Kit (Pierce). 20 μg samples from cellular fractions or 13.5 μg samples from nerve lysates were combined with SDS loading buffer (Life Technologies) and β-mercaptoethanol (MP Biomedicals, Santa Ana, CA) and incubated at 99 °C for 5 min. The samples were electrophoresed on 4–20% Tris-Glycine gels (Life Technologies) at 125V for 3 h in running buffer containing SDS (Life Technologies) at 4 °C. Protein samples were transferred onto PVDF membranes at 25 V for 1.5 h in Tris-Glycine Transfer Buffer (Life Technologies). Membranes were blocked in 2% non-fat milk in TBST overnight at 4 °C. Primary antibodies included: rabbit anti-GFP (1:2000, Sigma), mouse anti-JUN (1:500, BD Biosciences, San Jose, CA), rabbit anti-RAB7 (1:1000, Sigma), rabbit anti-MTMR2 [1:250, (46)], mouse anti-MTMR2 (1:5000, Abnova), or rabbit anti-MTMR2 [1:1000, (47)] and were applied in blocking solution for 1 h at room temperature. Membranes were washed 3 times with TBST, incubated for 1 h at room temperature with an anti-mouse or anti-rabbit secondary antibody conjugated to horseradish peroxidase (Millipore, Billerica, MA), washed three times with TBST, and incubated with SuperSignal West Dura substrate (Thermo Scientific) according to manufacturer's instructions.

siRNA transfections and qRT-PCR

Control siRNA (siControl 1, Ambion catalogue number AM4611) or Sox10 siRNA (siSox10 1, Ambion catalogue number s131239) were transfected into S16 or primary rat Schwann cells (48) using the Amaxa Nucleofection system following the manufacturer's instructions. At 48 h post-transfection, RNA was isolated using Tri-Reagent (Ambion) and analysed by quantitative RT-PCR. The relative amounts of each *Mtmr2* isoform were determined by the comparative Ct method and normalized to 18S rRNA. The sequences of the primers used for qRT-PCR are as follows: 18S rRNA, 5'-CGCCGCTAGAGGTGAAATTCT-3' and 5'-CCAACCTCCGACTTTCGTTCT-3'; *Mtmr2* Exon1A, 5'-GAGGAC TCACTGTCCAGCCAAA-3' and 5'-TTTGTGACAGTCAGCGTCCCT-3'; *Mtmr2* Exon1B, 5'-GAAATTGAATTGGCAGTGAAAA-3', and 5'-TACAGCACCAGTGAACGGAC -3'. To study the developmental regulation of *Mtmr2* mRNA isoforms, the above primers were used in qRT-PCR assays on cDNA samples generated from RNA isolated from P1 and P15 rat sciatic nerves.

Micrococcal nucleases (MNase)-aided chromatin immunoprecipitation (ChIP) *in vivo*

Snap-frozen sciatic nerves (P30) were ground and incubated in 1 ml of lysis buffer (50 mM Hepes–KOH, pH 7.5; 140 mM NaCl; 4 mM MgCl2; 10% Glycerol; 0.5% Igepal CA-630; 0.25% Triton X-100; Protease Inhibitor Cocktail) (49) rotating for 20 min at 4 °C. After 15 strokes with a Dounce homogenizer, samples were centrifuged at 18,000 x rcf for 10 min at 4 °C. Pellets were washed with 1 ml of MNase digestion buffer (0.32 M sucrose; 50 mM Tris-HCl, pH 7.5; 4 mM MgCl2; 1 mM CaCl2; Protease Inhibitor Cocktail) (50). Insoluble material was pelleted by centrifugation, samples were resuspended in 200 μl of MNase digestion buffer, and were incubated with 1 μl (2000 gel units) of MNase (New England Biolabs, M0247) for 7 min at 37 °C. Digestion was terminated by the addition of EDTA to a final concentration of 0.05 M. Samples were centrifuged at 18,000 x rcf for 20 min at 4 °C, and supernatants containing small fragments of chromatin were pooled. The majority of digested chromatin was about 150 base pairs in length (data not shown). ~1.5 μg of chromatin DNA was mixed with 5 μg of anti-H3K4me3 antibody (Millipore 04-745) in ChIP incubation buffer (50 mM NaCl; 50 mM Tris-HCl, pH 7.5; Protease Inhibitor Cocktail; 5 mM EDTA) with a final volume of 1 mL. Samples were allowed to incubate for 12–16 h at 4 °C on a rotator. 60 μl of Dynabeads Protein G (Invitrogen, 10004D) slurry was washed twice with 0.5% BSA in PBS and then incubated with each ChIP sample for 4 h at 4 °C on a rotator. ChIP samples were washed with washing buffer 1 (WB1, 50 mM Tris-HCl, pH7.5; 10 mM EDTA; 125 mM NaCl) once, WB2 (50 mM Tris-HCl, pH7.5; 10 mM EDTA; 250 mM NaCl) once, and WB3 (50 mM Tris-HCl, pH7.5; 10 mM EDTA; 500 mM NaCl) twice. The samples were eluted at 65 °C with elution buffer (50 mM NaCl; 50 mM Tris-HCl, pH 7.5; 5mM EDTA; 1% SDS) for 15 min. DNA was purified by phenol chloroform extraction and subjected to sequencing.

Supplementary Material

Supplementary Material is available at *HMG* online.

Acknowledgements

The authors thank Alessandra Bolino for mouse tissue and patient DNA samples, C. Yan Cheng and Fred Robinson for anti-MTMR2 antibodies, Miriam Meisler for RNA isolated from adult mouse brain, Sundeep Kalantry for RNA isolated from mouse brains at P3, Shigeki Iwase for RNA isolated from mouse brains at E16.5, Laurie Griffin for assistance counting cells and puncta, Chetna Gopinath for assistance with 5'RACE experiments, Shelley Almburg and Sasha Meshinchi for assistance with confocal microscopy, and Ken Inoue and Jim Lupski for wild-type and dominant-negative SOX10 expression constructs.

Conflict of Interest statement. None declared.

Funding

This work was supported by a Sir Keith Murdoch Fellowship from the American Australian Association to M.H.B.; University of Michigan Rackham Graduate School Regents Fellowship to E.A.F.; a National Science Foundation Pre-Doctoral Fellowship to J.F.R-.M.; the National Institutes of Health Genetics Training Grant [GM007544 supporting W.D.L.]; and the National Institute of Neurological Diseases and Stroke [NS073748 to A.A. and NS083841 to J.S.].

References

1. Skre, H. (1974) Genetic and clinical aspects of Charcot-Marie-Tooth's disease. *Clin Genet.*, **6**, 98–118.

2. Dyck, P.J. and Lambert, E.H. (1968) Lower motor and primary sensory neuron diseases with peroneal muscular atrophy. II. Neurologic, genetic, and electrophysiologic findings in various neuronal degenerations. *Arch. Neurol.*, **18**, 619–625.
3. Dyck, P.J. and Lambert, E.H. (1968) Lower motor and primary sensory neuron diseases with peroneal muscular atrophy. I. Neurologic, genetic, and electrophysiologic findings in hereditary polyneuropathies. *Arch. Neurol.*, **18**, 603–618.
4. Monk, K.R., Feltri, M.L. and Taveggia, C. (2015) New insights on Schwann cell development. *Glia*, **63**, 1376–1393.
5. Harding, A.E. and Thomas, P.K. (1980) The clinical features of hereditary motor and sensory neuropathy types I and II. *Brain*, **103**, 259–280.
6. Brennan, K.M., Bai, Y. and Shy, M.E. (2015) Demyelinating CMT-what's known, what's new and what's in store? *Neurosci. Lett.*, **596**, 14–26.
7. Su, Y., Brooks, D.G., Li, L., Lepercq, J., Trofatter, J.A., Ravetch, J.V. and Lebo, R.V. (1993) Myelin protein zero gene mutated in Charcot-Marie-tooth type 1B patients. *Proc. Natl Acad. Sci. U S A*, **90**, 10856–10860.
8. Warner, L.E., Mancias, P., Butler, I.J., McDonald, C.M., Keppen, L., Koob, K.G. and Lupski, J.R. (1998) Mutations in the early growth response 2 (EGR2) gene are associated with hereditary myelinopathies. *Nat. Genet.*, **18**, 382–384.
9. Bolino, A., Muglia, M., Conforti, F.L., LeGuern, E., Salih, M.A., Georgiou, D.M., Christodoulou, K., Hausmanowa-Petrusewicz, I., Mandich, P., Schenone, A., *et al.* (2000) Charcot-Marie-Tooth type 4B is caused by mutations in the gene encoding myotubularin-related protein-2. *Nat. Genet.*, **25**, 17–19.
10. Gambardella, A., Bono, F., Muglia, M., Valentino, P. and Quattrone, A. (1999) Autosomal recessive hereditary motor and sensory neuropathy with focally folded myelin sheaths (CMT4B). *Ann. N Y Acad. Sci.*, **883**, 47–55.
11. Bolis, A., Coviello, S., Bussini, S., Dina, G., Pardini, C., Previtali, S.C., Malaguti, M., Morana, P., Del Carro, U., Feltri, M.L., *et al.* (2005) Loss of Mtmr2 phosphatase in Schwann cells but not in motor neurons causes Charcot-Marie-Tooth type 4B1 neuropathy with myelin outfoldings. *J. Neurosci.*, **25**, 8567–8577.
12. Patzig, J., Jahn, O., Tenzer, S., Wichert, S.P., de Monasterio-Schrader, P., Rosfa, S., Kuharev, J., Yan, K., Bormuth, I., Bremer, J., *et al.* (2011) Quantitative and integrative proteome analysis of peripheral nerve myelin identifies novel myelin proteins and candidate neuropathy loci. *J. Neurosci.*, **31**, 16369–16386.
13. Chojnowski, A., Ravise, N., Bachelin, C., Depienne, C., Ruberg, M., Brugg, B., Laporte, J., Baron-Van Evercooren, A. and LeGuern, E. (2007) Silencing of the Charcot-Marie-Tooth associated MTMR2 gene decreases proliferation and enhances cell death in primary cultures of Schwann cells. *Neurobiol. Dis.*, **26**, 323–331.
14. Vaccari, I., Dina, G., Tronchere, H., Kaufman, E., Chicanne, G., Cerri, F., Wrabetz, L., Payrastre, B., Quattrini, A., Weisman, L.S., *et al.* (2011) Genetic interaction between MTMR2 and FIG4 phospholipid phosphatases involved in Charcot-Marie-Tooth neuropathies. *PLoS Genet.*, **7**, e1002319.
15. Berger, P., Bonneick, S., Willi, S., Wymann, M. and Suter, U. (2002) Loss of phosphatase activity in myotubularin-related protein 2 is associated with Charcot-Marie-Tooth disease type 4B1. *Hum. Mol. Genet.*, **11**, 1569–1579.
16. Begley, M.J. and Dixon, J.E. (2005) The structure and regulation of myotubularin phosphatases. *Curr. Opin. Struct .Biol.*, **15**, 614–620.
17. Bolis, A., Zordan, P., Coviello, S. and Bolino, A. (2007) Myotubularin-related (MTMR) phospholipid phosphatase proteins in the peripheral nervous system. *Mol. Neurobiol.*, **35**, 308–316.
18. Previtali, S.C., Zerega, B., Sherman, D.L., Brophy, P.J., Dina, G., King, R.H., Salih, M.M., Feltri, L., Quattrini, A., Ravazzolo, R., *et al.* (2003) Myotubularin-related 2 protein phosphatase and neurofilament light chain protein, both mutated in CMT neuropathies, interact in peripheral nerve. *Hum. Mol. Genet.*, **12**, 1713–1723.
19. Bremer, M., Frob, F., Kichko, T., Reeh, P., Tamm, E.R., Suter, U. and Wegner, M. (2011) Sox10 is required for Schwann-cell homeostasis and myelin maintenance in the adult peripheral nerve. *Glia*, **59**, 1022–1032.
20. Antonellis, A. and Green, E.D. (2008) Willard, H. and Ginsburg, G. (eds.), In *Genomic and Personalized Medicine*. Academic Press, Salt Lake City, in press., pp. 120–130.
21. Kent, W.J., Sugnet, C.W., Furey, T.S., Roskin, K.M., Pringle, T.H., Zahler, A.M. and Haussler, D. (2002) The human genome browser at UCSC. *Genome Res.*, **12**, 996–1006.
22. Goda, S., Hammer, J., Kobiler, D. and Quarles, R.H. (1991) Expression of the myelin-associated glycoprotein in cultures of immortalized Schwann cells. *J. Neurochem.*, **56**, 1354–1361.
23. Hai, M., Muja, N., DeVries, G.H., Quarles, R.H. and Patel, P.I. (2002) Comparative analysis of Schwann cell lines as model systems for myelin gene transcription studies. *J. Neurosci. Res.*, **69**, 497–508.
24. Hodonsky, C.J., Kleinbrink, E.L., Charney, K.N., Prasad, M., Bessling, S.L., Jones, E.A., Srinivasan, R., Svaren, J., McCallion, A.S. and Antonellis, A. (2012) SOX10 regulates expression of the SH3-domain kinase binding protein 1 (Sh3kbp1) locus in Schwann cells via an alternative promoter. *Mol. Cell Neurosci.*, **49**, 85–96.
25. Antonellis, A., Bennett, W.R., Menheniott, T.R., Prasad, A.B., Lee-Lin, S.Q., Green, E.D., Paisley, D., Kelsh, R.N., Pavan, W.J. and Ward, A. (2006) Deletion of long-range sequences at Sox10 compromises developmental expression in a mouse model of Waardenburg-Shah (WS4) syndrome. *Hum. Mol. Genet.*, **15**, 259–271.
26. Salazar-Grueso, E.F., Kim, S. and Kim, H. (1991) Embryonic mouse spinal cord motor neuron hybrid cells. *Neuroreport.*, **2**, 505–508.
27. Bolino, A., Marigo, V., Ferrera, F., Loader, J., Romio, L., Leoni, A., Di Duca, M., Cinti, R., Cecchi, C., Feltri, M.L., *et al.* (2002) Molecular characterization and expression analysis of Mtmr2, mouse homologue of MTMR2, the Myotubularin-related 2 gene, mutated in CMT4B. *Gene*, **283**, 17–26.
28. Yaffe, D. and Saxel, O. (1977) Serial passaging and differentiation of myogenic cells isolated from dystrophic mouse muscle. *Nature*, **270**, 725–727.
29. Suter, U., Snipes, G.J., Schoener-Scott, R., Welcher, A.A., Pareek, S., Lupski, J.R., Murphy, R.A., Shooter, E.M. and Patel, P.I. (1994) Regulation of tissue-specific expression of alternative peripheral myelin protein-22 (PMP22) gene transcripts by two promoters. *J. Biol. Chem.*, **269**, 25795–25808.
30. Franklin, N.E., Taylor, G.S. and Vacratsis, P.O. (2011) Endosomal targeting of the phosphoinositide 3-phosphatase MTMR2 is regulated by an N-terminal phosphorylation site. *J. Biol. Chem.*, **286**, 15841–15853.
31. Lopez-Anido, C., Sun, G., Koenning, M., Srinivasan, R., Hung, H.A., Emery, B., Keles, S. and Svaren, J. (2015) Differential Sox10 genomic occupancy in myelinating glia. *Glia*, **63**, 1897–1914.

32. Jones, E.A., Jang, S.W., Mager, G.M., Chang, L.W., Srinivasan, R., Gokey, N.G., Ward, R.M., Nagarajan, R. and Svaren, J. (2007) Interactions of Sox10 and Egr2 in myelin gene regulation. *Neuron Glia Biol.*, **3**, 377–387.
33. Srinivasan, R., Sun, G., Keles, S., Jones, E.A., Jang, S.W., Krueger, C., Moran, J.J. and Svaren, J. (2012) Genome-wide analysis of EGR2/SOX10 binding in myelinating peripheral nerve. *Nucleic Acids Res.*, **40**, 6449–6460.
34. Harley, V.R., Lovell-Badge, R. and Goodfellow, P.N. (1994) Definition of a consensus DNA binding site for SRY. *Nucleic Acids Res.*, **22**, 1500–1501.
35. Peirano, R.I. and Wegner, M. (2000) The glial transcription factor Sox10 binds to DNA both as monomer and dimer with different functional consequences. *Nucleic Acids Res.*, **28**, 3047–3055.
36. Stolt, C.C. and Wegner, M. (2010) SoxE function in vertebrate nervous system development. *Int. J. Biochem. Cell Biol.*, **42**, 437–440.
37. Inoue, K., Khajavi, M., Ohyama, T., Hirabayashi, S., Wilson, J., Reggin, J.D., Mancias, P., Butler, I.J., Wilkinson, M.F., Wegner, M., *et al.* (2004) Molecular mechanism for distinct neurological phenotypes conveyed by allelic truncating mutations. *Nat. Genet.*, **36**, 361–369.
38. Laporte, J., Blondeau, F., Buj-Bello, A. and Mandel, J.L. (2001) The myotubularin family: from genetic disease to phosphoinositide metabolism. *Trends Genet.*, **17**, 221–228.
39. Weider, M., Reiprich, S. and Wegner, M. (2013) Sox appeal - Sox10 attracts epigenetic and transcriptional regulators in myelinating glia. *Biol. Chem.*, **394**, 1583–1593.
40. Houlden, H., Girard, M., Cockerell, C., Ingram, D., Wood, N.W., Goossens, M., Walker, R.W. and Reilly, M.M. (2004) Connexin 32 promoter P2 mutations: a mechanism of peripheral nerve dysfunction. *Ann. Neurol.*, **56**, 730–734.
41. Antonellis, A., Dennis, M.Y., Burzynski, G., Huynh, J., Maduro, V., Hodonsky, C.J., Khajavi, M., Szigeti, K., Mukkamala, S., Bessling, S.L., *et al.* (2010) A rare myelin protein zero (MPZ) variant alters enhancer activity in vitro and in vivo. *PLoS One*, **5**, e14346.
42. Brewer, M.H., Ma, K.H., Beecham, G.W., Gopinath, C., Baas, F., Choi, B.O., Reilly, M.M., Shy, M.E., Zuchner, S., Svaren, J., *et al.* (2014) Haplotype-specific modulation of a SOX10/CREB response element at the Charcot-Marie-Tooth disease type 4C locus SH3TC2. *Hum. Mol. Genet.*, **23**, 5171–5187.
43. Kurihara, T., Monoh, K., Sakimura, K. and Takahashi, Y. (1990) Alternative splicing of mouse brain 2',3'-cyclic-nucleotide 3'-phosphodiesterase mRNA. *Biochem. Biophys. Res. Commun.*, **170**, 1074–1081.
44. Söhl, G., Gillen, C., Bosse, F., Gleichmann, M., Müller, H.W. and Willecke, K. (1996) A second alternative transcript of the gap junction gene connexin32 is expressed in murine Schwann cells and modulated in injured sciatic nerve. *Eur. J. Cell Biol.*, **69**, 267–275.
45. Guo, F., Chiang, M.Y., Wang, Y. and Zhang, Y.Z. (2008) An in vitro recombination method to convert restriction- and ligation-independent expression vectors. *Biotechnol J.*, **3**, 370–377.
46. Li, J.C., Samy, E.T., Grima, J., Chung, S.S., Mruk, D., Lee, W.M., Silvestrini, B. and Cheng, C.Y. (2000) Rat testicular myotubularin, a protein tyrosine phosphatase expressed by Sertoli and germ cells, is a potential marker for studying cell-cell interactions in the rat testis. *J. Cell Physiol.*, **185**, 366–385.
47. Ng, A.A., Logan, A.M., Schmidt, E.J. and Robinson, F.L. (2013) The CMT4B disease-causing phosphatases Mtmr2 and Mtmr13 localize to the Schwann cell cytoplasm and endomembrane compartments, where they depend upon each other to achieve wild-type levels of protein expression. *Hum. Mol. Genet.*, **22**, 1493–1506.
48. Gokey, N.G., Srinivasan, R., Lopez-Anido, C., Krueger, C. and Svaren, J. (2012) Developmental regulation of microRNA expression in Schwann cells. *Mol. Cell Biol.*, **32**, 558–568.
49. Schmidt, D., Wilson, M.D., Spyrou, C., Brown, G.D., Hadfield, J. and Odom, D.T. (2009) ChIP-seq: using high-throughput sequencing to discover protein-DNA interactions. *Methods*, **48**, 240–248.
50. Umlauf, D., Goto, Y. and Feil, R. (2004) Site-specific analysis of histone methylation and acetylation. *Methods Mol. Biol.*, **287**, 99–120.